

# 2×2 Electro-optic Switch with fJ/bit Switching Power Based on Dual Photonic Crystal Nanobeam Cavities

Huanying Zhou<sup>1</sup>, Ciyuan Qiu<sup>1,\*</sup>, Jiayang Wu<sup>1</sup>, Boyu Liu<sup>1</sup>, Xinhong Jiang<sup>1</sup>, Jizong Peng<sup>1</sup>, Zhenzhen Xu<sup>1</sup>, Yong Zhang<sup>1</sup>, Ruili Liu<sup>1</sup>, Yikai Su<sup>1,\*</sup>, and Richard Soref<sup>2</sup>

<sup>1</sup>State Key Laboratory of Advanced Optical Communication Systems and Networks, Department of Electronic Engineering, Shanghai Jiao Tong University, 800 Dongchuan Rd, Shanghai, 200240, China

<sup>2</sup>Engineering Department, University of Massachusetts, Boston, Massachusetts, 02125, USA

\*Corresponding author: [qiuciyuan@sjtu.edu.cn](mailto:qiuciyuan@sjtu.edu.cn)

**Abstract:** We propose a compact ( $5\ \mu\text{m}\times 40\ \mu\text{m}$ )  $2\times 2$  electro-optic switch implemented by dual silicon photonic crystal nanobeam (PCN) cavities. A switching power of 2.6 fJ/bit is numerically demonstrated. Extinction ratios of 14.2/13.4 dB are achieved at through/drop ports.

**OCIS codes:** (130.3120) Integrated optics devices; (230.5298) Photonic crystals; (130.4815) Optical switching devices

## 1. Introduction

Optical switches are key building blocks for optical communication networks. Ever-increasing network capacity and large-scale on-chip integration are driving the demand for low-power electro-optic (EO) switches with small device footprints. In previous reports, various schemes have been demonstrated to implement EO switches based on silicon microring resonators (MRRs) [1], and Mach-Zehnder interferometers (MZIs) [2]. However, MRRs and MZIs have physical lengths of several tens or even hundreds of micrometers, leading to relatively large device footprints and high power dissipation caused by free carrier absorption (FCA) in these EO switches.

In recent years, photonic crystal nanobeam (PCN) cavities have attracted considerable attention for implementing many new optoelectronic devices, including optical filters, EO modulators and so on [3–6]. In the PCN cavity, photons are strongly confined within a small mode volume and light-material interaction is highly enhanced [7,8]. Since the mode volume and light-matter interaction have effect on the switching energy [4,9], EO switches based on PCN cavities could significantly reduce device footprints and power consumption. In this paper, for the first time to the best of our knowledge, a scheme to implement an ultra-low power  $2\times 2$  EO switch based on dual PCN cavities is proposed. Based on the finite-difference-time-domain (FDTD) method, extinction ratios of 14.2/13.4 dB at through/drop ports are obtained in the EO switching and the switching power is calculated to be 2.6 fJ/bit.

## 2. Device structure and operation principle

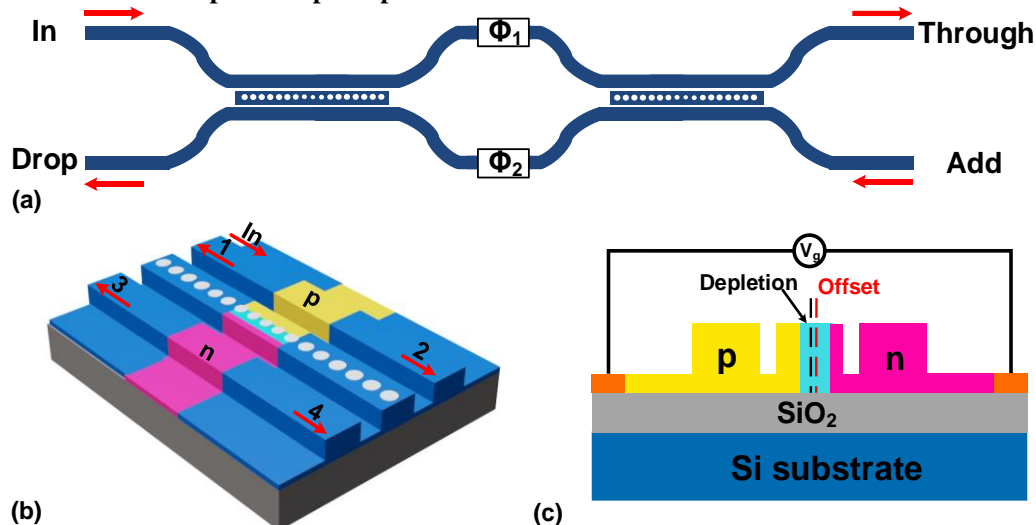


Fig. 1. (a) Schematic diagram of the  $2\times 2$  EO switch based on dual PCN cavities. The phase difference between the two arms ( $\Phi_1-\Phi_2$ ) is equal to  $\pi$ . (b) Schematic perspective view of a single PCN cavity with an embedded PN junction. (c) Cross-section view of the PN junction.

The proposed  $2\times 2$  silicon EO switch is a compact four-port system consisting of two cascaded identical PCN cavities, as illustrated in Fig. 1(a). The schematic perspective view of a single PCN cavity is shown in Fig. 1(b). In the PCN cavity, the central nanobeam waveguide of  $0.565\ \mu\text{m}$  width is evanescently coupled to two identical bus waveguides of  $0.6\ \mu\text{m}$  width. The height of the rib waveguide is 220 nm and the thickness of the slab is 50 nm. The

central nanobeam waveguide etched by an array of air-holes can form a Fabry-Perot (F-P) cavity, which consists of a central-taper section and two side-reflector sections. The central-taper section with 13 holes is optimized to reduce the scattering losses and provide high phase matching between the photonic crystal Bloch mode and the waveguide mode. The side-reflector sections are designed as two mirrors to reflect light to the central-taper section [6]. TE polarization is used in the simulation. To realize high drop transmission at the cross state [3,10], a  $\pi$ -phase difference between the two arms ( $\Phi_1 - \Phi_2$ ) is achieved by tuning the silicon refractive index. Note that the phase difference can also be introduced by changing the length of the two arms.

Identical PN junctions are embedded on the two PCN cavities respectively to achieve EO tuning. The cross-section view of the PN junction is shown in Fig. 1(c). The doping concentration is  $1 \times 10^{18} \text{ cm}^{-3}$  in the n-type region while it is  $5 \times 10^{17} \text{ cm}^{-3}$  in the p-type region. The complex refractive index for the n-type doping regions and p-type doping regions are set to be  $n = 3.474148$ ,  $k = 0.000112$  and  $n = 3.473960$ ,  $k = 0.000031$ , respectively [11]. In order to maximize the carrier-photon overlap and reduce the energy loss, a PN junction positional offset about 100 nm is introduced. If a bias voltage is applied on the PN junction, the width of the depletion region can be changed [12]. Then the refractive index of the silicon nanobeam waveguide is tuned. Thus both the resonance wavelength and quality factor of the nanobeam cavity can be changed and EO switching is obtained. Since the optical intensity is highly confined in the center of the nanobeam cavity, the length of the PN junction is set to be 2  $\mu\text{m}$ .

### 3. Simulation Results

The passive device without PN junction is firstly characterized. The normalized transmission spectra of a single PCN cavity is shown in Fig. 2(a), the transmission efficiency at each port is about 25%, thus  $\sim 6$  dB extinction ratio is achieved at the through port [5]. Fig. 2(b) shows the normalized transmission spectra of the  $2 \times 2$  switch based on two PCN cavities. A 19.2 dB extinction ratio is obtained in the through port (red line). The drop efficiency is about 89% at the resonance wavelength (blue line). The full-width-half-maximum (FWHM) of the drop port spectrum is  $\sim 0.18$  nm with a quality factor of  $\sim 9000$ , which is depicted in the inset of Fig. 2(b).

In the EO switching, for the device with integrated PN junctions, the same bias voltages are applied simultaneously on the two PCN cavities. If 0.89 V is applied, the width of the depletion region of the PN junction is 10 nm. The transmission spectra at through port and drop port are shown as red and blue lines in Fig. 2(c), respectively. If the bias voltage is decreased to  $-2.79$  V, the free carriers are swept out of the waveguide and the width of the depletion region is increased to 120 nm. The effective index of the silicon waveguide is increased thus the transmission spectra red shifts  $\sim 0.8$  nm. Here the input wavelength is 1621.53 nm which is the same as the resonance wavelength at a bias voltage of 0.89 V. Then  $\sim 75\%$  of the input optical power goes to the drop port and the device work at the cross state if the bias voltage is 0.89 V. The switch is changed to the bar state and  $\sim 91\%$  of the optical power goes to the through port if the bias voltage is  $-2.79$  V. As shown in Fig. 2(c), at the through/drop ports, 14.2/13.4 dB extinction ratios are achieved and the switching power is calculated to be about 2.6 fJ/bit [12].

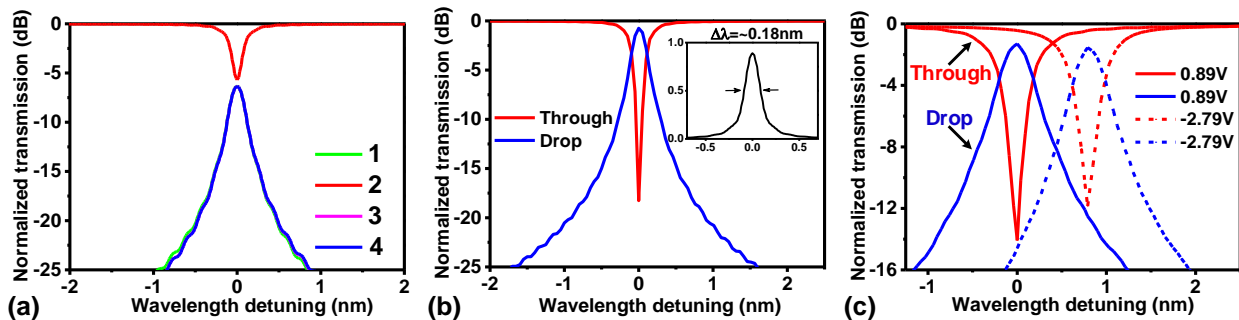


Fig. 2. (a) Normalized transmission spectra of a single PCN. (b) Normalized transmission spectra of the device without PN junction in through (red line)/drop (blue line) ports, the inset shows the drop transmission spectrum with a FWHM of  $\sim 0.18$  nm. (c) Normalized transmission spectra of the device under different bias voltages.

### 4. Conclusion

In conclusion, a compact  $2 \times 2$  EO switch based on dual silicon PCN cavities has been proposed. It has a compact device footprint of  $5 \mu\text{m} \times 40 \mu\text{m}$  and an ultra-low switching power of 2.6 fJ/bit. Extinction ratios of 14.2/13.4 dB at through/drop ports are also achieved in the simulation.

### 5. References

- [1] H. Lira, *et al.*, Opt. Express. **17**, 22271 (2009).
- [2] P. Dong, *et al.*, Opt. Express. **18**, 25225 (2010).
- [3] C. Poulton, *et al.*, Opt. Lett. **40**, 4206 (2015).
- [4] B. Schmidt, *et al.*, Opt. Express. **15**, 3140 (2007).
- [5] X. Ge, *et al.*, Opt. Lett. **39**, 6973 (2014).
- [6] T. Pan, *et al.*, Opt. Express. **23**, 23357 (2015).
- [7] Q. Quan, *et al.*, Opt. Express **19**, 18529 (2011).
- [8] W. Fegadolli, *et al.*, Opt. Express. **21**, 3861 (2013).
- [9] K. Nozaki, *et al.*, Opt. Express. **4**, 477 (2010).
- [10] C. Manolatou, *et al.*, IEEE J. Quant. Electron. **35**, 1322 (1999).
- [11] R. Soref, *et al.*, IEEE J. Quant. Electron. **23**, 123 (1987).
- [12] J. Hendrickson, *et al.*, Opt. Express. **22**, 3271 (2014).